Light-Induced Torque in Ferromagnetic Metals via Orbital Angular Momentum Generated by Photon Helicity

Koki Nukui,[1,2] Satoshi Iihama,[3,2,*,‡] Kazuaki Ishibashi,[1,2] Shogo Yamashita,[1] Akimasa Sakuma,[1] Philippe Scheid,[4] Grégory Malinowski,[4] Michel Hehn,[4,5] Stéphane Mangin,[4,5] and Shigemi Mizukami[2,5,†]

[1]*Department of Applied Physics, Graduate School of Engineering, Tohoku University, Sendai 980-8579, Japan*
[2]*WPI Advanced Institute for Materials Research (AIMR), Tohoku University, 2-1-1, Katahira, Sendai 980-8577, Japan*
[3]*Frontier Research Institute for Interdisciplinary Sciences (FRIS), Tohoku University, Sendai 980-8578, Japan*
[4]*Université de Lorraine, CNRS, Institut Jean Lamour, F-54000 Nancy, France*
[5]*Center for Science and Innovation in Spintronics (CSIS), Tohoku University, Sendai 980-8577, Japan*

(Received 10 May 2024; revised 25 August 2024; accepted 15 November 2024; published 2 January 2025)

We investigated photon-helicity–induced magnetization precession in $Co_{1-x}Pt_x$ alloy thin films. In addition to field-like torque, attributable to magnetic field generation owing to the "inverse Faraday effect," we observed nontrivial and large damping-like torque that has never been discussed for single ferromagnetic layer. The composition dependence of these two torques is effectively elucidated by a model that considers mutual coupling via spin-orbit interaction between magnetization and the electronic orbital angular momentum generated by photon helicity. This Letter significantly enhances our understanding of the physics relevant to the interplay of photon helicity and magnetization in magnetic metals.

DOI: 10.1103/PhysRevLett.134.016701

Photon carries both spin and orbital angular momenta, in circularly polarized and vortex electromagnetic waves, respectively, and utilization of these angular momentum of photons is one issue in modern physics [1,2]. Considerable attention has been devoted in condensed matter physics to the interaction between photons' angular momentum and matter, fostering technological advances such as vortex nanoprocessing [3,4] and optical information communications [5–7].

Intriguing physical phenomena relevant to the angular momentum of photon are also discussed as one of the central subjects in optomagnetism. The "inverse Faraday effect" is a physical phenomenon in which magnetization $\mathbf{M}_p$ or magnetic field $\mathbf{H}_p$ emerges during the dwell time when circularly polarized light passes through a dielectric medium, and it can be expressed as

$$\mathbf{M}_p, \mathbf{H}_p \propto \mathbf{E}(\omega_p) \times \mathbf{E}^{\star}(\omega_p), \tag{1}$$

where $\mathbf{E}$ is electric field vector for light with an angular frequency of ω_p [8,9]. $\mathbf{H}_p$ can be generated instantaneously when light is irradiated on magnetic dielectric materials owing to magneto-optical coupling such as the magneto-optical Faraday effect [10]. Consequently, GHz-to-THz dynamics of magnetic order are initiated when a circularly polarized femtosecond laser pulse passes through magnetic materials via the inverse Faraday effect, enabling us to explore various spin dynamics along with various probes. This is an ultrafast and versatile modern technique [11–16].

The inverse Faraday effect has also been discussed in magnetic metals and a highlight is circularly polarized laser pulse-induced magnetization reversal, commonly referred to as all-optical helicity dependent switching, partially attributed to the inverse Faraday effect [17–23]. Considerable efforts have been devoted to understanding the physics of the inverse Faraday effect in metals; however, there is still a notable gap in our understanding of the key physics—for example, the nature of magnetization arising from the inverse Faraday effect in metallic ferromagnets. A recent study discussed the inverse Faraday effect in terms of the above-mentioned effective magnetic field to interpret the light-induced precessional magnetization dynamics observed in various ferromagnets and normal metal bilayers [14,24–28]. Many theories reported light-induced magnetization of metals [29–37]. According to the recent theoretical analysis of the inverse Faraday effect magnetization, $\mathbf{M}_p$ in metals predominantly consists of orbital angular momentum (OAM) and not spin angular momentum (SAM) [29]. On the other hand, in addition to the inverse Faraday effect, both OAM and SAM can be induced as an absorbed quantity [35,37–39]. Although the inverse Faraday effect is proportional to the laser intensity, i.e., the effect vanishes after the laser passes away from the matter, OAM and SAM are induced by the absorption of photonic angular momentum that remains in matter even after the laser passes away from it. By using the absorption,

*Contact author: iihama.satoshi.y0@f.mail.nagoya-u.ac.jp
†Contact author: shigemi.mizukami.a7@tohoku.ac.jp
‡Present address: Department of Materials Physics, Nagoya University, Nagoya 464-8603, Japan.

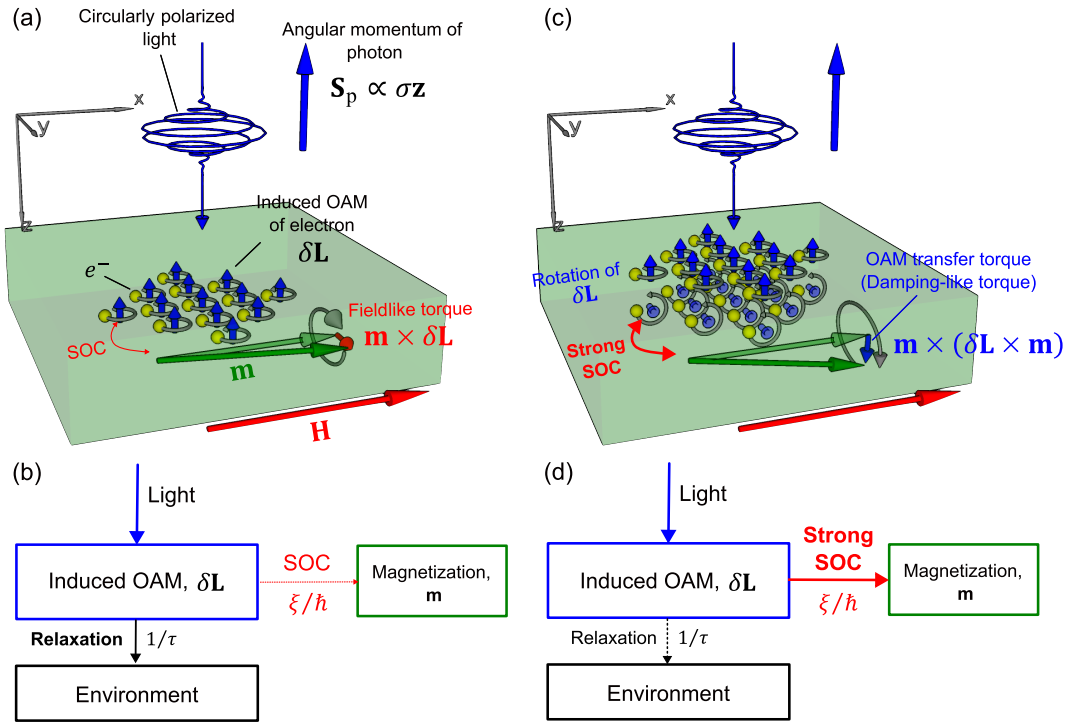

FIG. 1. (a),(c) Schematic illustration of photon-helicity generated OAM of electron and magnetization dynamics excitation. Circularly polarized light has an angular momentum where its sign depends on helicity (σ). The OAM ($\delta\mathbf{L}$) is generated parallel to $\mathbf{S}_p$. Magnetization dynamics are excited by SOC. Schematic of angular momentum flow induced by photon helicity when (b) relaxation to the environment is stronger than SOC and when (d) SOC is stronger than relaxation to environment. When angular momentum flow through SOC dominates over relaxation to environment, $\delta\mathbf{L}$ rotates within laser pulse duration; then, magnetization dynamics can be excited by OAM transfer torque as shown in (c).

OAM can be induced in any dissipative materials. It is then intriguing to determine whether the light-induced angular momentum in metals is relevant to orbital magnetism in the context of recent research on the magnetization dynamics induced by an electric field (current) via OAM [40–46]. Furthermore, their deep understanding will also push technologies relevant to optomagnetism, such as the aforementioned all-optical helicity dependent switching.

In this Letter, we elucidate the role of electronic OAM in the dynamics of magnetization induced by circularly polarized laser pulses in ferromagnets. Our experimental data clearly demonstrate the existence of not only the effective magnetic field, traditionally interpreted as the inverse Faraday effect, but also a nontrivial and large effective magnetic field that is orthogonal to that induced by the inverse Faraday effect. In other words, these correspond to the field and damping-like torques, respectively. In the former scenario, a circularly polarized laser pulse acts as an effective magnetic field that induces field-like torque. On the other hand, the latter scenario where damping-like torque is generated cannot be explained by the traditional inverse Faraday effect alone. Both torques can be understood with a simple model we provide, on an equal footing, that considers the nonequilibrium OAM induced by the angular momentum of a photon and its coupling with magnetization via spin-orbit interactions in ferromagnetic metals. Here, it should also be noted that the effective magnetic field generation in the model is different from the traditional model [Eq. (1)] in which magneto-optical coupling plays an important role.

As mentioned above, we focus on both kinds of torque (or effective magnetic field), and these are illustrated in Fig. 1. In Fig. 1, the macroscopic magnetization of a ferromagnetic metal film is in the film plane ($\mathbf{m} \| \mathbf{x}$) and circularly polarized laser pulse with $\mathbf{k}$ vector incidents along the film normal ($\mathbf{k} \| \mathbf{z}$). In this geometry, magnetization precession is induced and the initial phase is determined by the direction of the total torque. The absorption of photonic angular momentum induces $\mathbf{M}_p$ parallel to $\mathbf{z}$, which will then act on magnetization as an effective magnetic field, i.e., the field-like torque, via a coupling between $\mathbf{m}$ and $\mathbf{M}_p$, $\mathbf{T} \propto \mathbf{m} \times \mathbf{M}_p$ [Fig. 1(a)], as reported [14,24,27]. In the opposite case, the direction of the $\mathbf{M}_p$ changes owing to strong coupling between $\mathbf{M}_p$ and $\mathbf{m}$, leading to the emergence of the damping-like torque, i.e., $\mathbf{T} \propto \mathbf{m} \times (\mathbf{M}_p \times \mathbf{m})$ [Fig. 1(c)]. Hereafter, we assume that $\mathbf{M}_p$ is dominantly caused by the electronic OAM $\delta\mathbf{L}$ induced by light, as shown in Fig. 1. The path of the angular momentum flow is schematically shown in

Figs. 1(b) and 1(d). When relaxation to environment for induced OAM is stronger than the coupling with magnetization, light acts as the field-like torque [Figs. 1(a) and 1(b)]. However, coupling between induced OAM and magnetization is stronger than relaxation to environment, the damping-like torque as an OAM transfer torque is induced by light irradiation [Figs. 1(c) and 1(d)]. Consequently, the two cases are characterized by the coupling strength between $\mathbf{m}$ and $\delta\mathbf{L}$ and relaxation of $\delta\mathbf{L}$. In the realm of torque physics induced by the OAM generated by electric current or field, one can intuitively infer that the coupling strength between $\mathbf{m}$ and $\delta\mathbf{L}$ is governed by spin-orbital coupling (SOC), given that magnetization stems from SAM in transition metal ferromagnets. Hence, the field- and damping-like torques can be tuned by the heavy-metal addition into ferromagnetic metals.

Five-nanometer-thick $Co_{1-x}Pt_x$ alloy thin film samples with different compositions (x) were prepared by magnetron sputtering. The stacking structure of the sample is as follows: Si/SiO_2 sub./$Co_{1-x}Pt_x(5)/Al(2)$ (thickness is in nanometers). The wavelength and pulse duration of the pump and probe laser pulse used for the circularly polarized laser induced magnetization dynamics measurements were 800 nm and 100 fs, respectively. The pump fluence (F_p) used for the measurement was fixed at 4.6 J/m^2. An in-plane external magnetic field of 2 T was applied during the measurement. The measurement was performed at room temperature. Figure 2 shows the effect of left circularly polarized (LCP) and right circularly polarized (RCP) laser on normalized Kerr rotation angle $\Delta\theta_K/\theta_K$ to determine the impact on magnetization dynamics in Co [Fig. 2(a)] and $Co_{35}Pt_{65}$ alloy [Fig. 2(b)]. Magnetization precession was excited after irradiation with a femtosecond laser pulse. The oscillation phase reversed when the photon helicity was reversed, indicating a photon-helicity–induced torque on magnetization. The slightly different amplitudes between the irradiation of the LCP and RCP resulted from thermally induced magnetization precession, likely caused by a slight misalignment between the sample and the applied field. To extract the photon-helicity–induced signal, the normalized difference signal $[(\Delta\theta_K(\mathrm{RCP}) - \theta_K(\mathrm{LCP}))/(2\theta_K)]$ was taken as shown in Figs. 2(c) and 2(d). This photon-helicity–induced normalized change in the Kerr rotation angle was then fitted by the following equation:

$$f(t) = \left(\delta m_{z,\sin}\sin(2\pi f_0 t) + \delta m_{z,\cos}\cos(2\pi f_0 t)\right) \times \exp(-t/\tau_0), \quad (2)$$

where $\delta m_{z,\sin(\cos)}$, f_0, and τ_0 are sine (cosine) amplitude, frequency, and lifetime of magnetization precession, respectively. The broken and solid curves in Figs. 2(c) and 2(d) represent the fitted results based on Eq. (2). In the case of Co, the magnetization precession excited by the photon helicity was sinelike, indicating that the field-like torque was dominant. In contrast, a phase shift and cosine-like components, which are signatures of the damping-like torque, were exhibited by the $Co_{35}Pt_{65}$ alloy.

Figure 3(a) shows $\delta m_{z,\sin}$ and $\delta m_{z,\cos}$ plotted as functions of the Pt composition (x). Both values increased with increasing x. In particular, a relatively significant increase of $\delta m_{z,\cos}$ was observed with an increase in x, compared with that of $\delta m_{z,\sin}$. The relative magnitudes of two values significantly changed, resulting in a change in the initial phase $\varphi(=\tan^{-1}(\delta m_{z,\cos}/\delta m_{z,\sin}))$ [Fig. 3(b)]. This phase change indicates that the damping-like torque enhances with increasing Pt concentration in $Co_{1-x}Pt_x$, and therefore the SOC correlates with the above-mentioned physical scenario relevant to the OAM.

For a more quantitative discussion of both amplitudes (δm_z) and phase change (φ), we consider the physics based

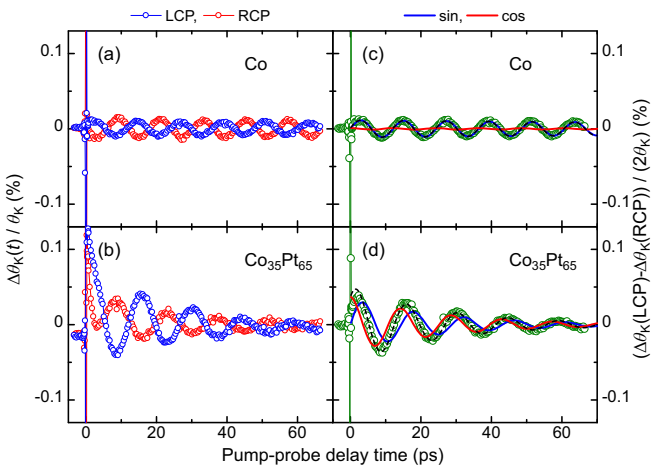

FIG. 2. (a) and (b) Circularly polarized laser pulse-induced change in normalized Kerr rotation angle $[\Delta\theta_K(t)/\theta_K]$ in Co and $Co_{35}Pt_{65}$ alloy films with different photon helicity using LCP and RCP laser pulses. (c),(d) Helicity-dependent change in normalized Kerr angle rotation $[(\Delta\theta_K(\mathrm{LCP}) - \Delta\theta_K(\mathrm{RCP}))/(2\theta_K)]$ as a function of time for Co and $Co_{35}Pt_{65}$ alloy films extracted from (a) and (b). Broken and solid curves are results fitted using a sinusoidal decayed function [Eq. (2)].

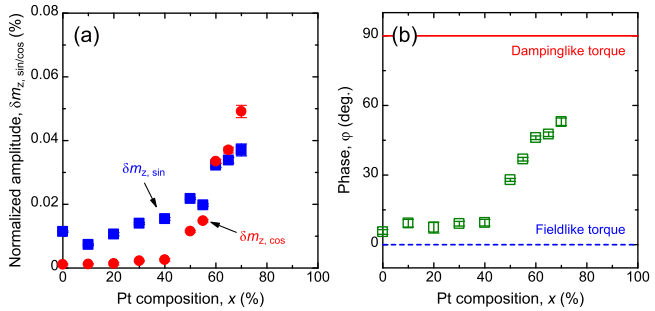

FIG. 3. (a) Photon-helicity–induced magnetization precession amplitude ($\delta m_{\sin}$ and $\delta m_{\cos}$) as a function of the Pt composition (x) in $Co_{1-x}Pt_x$ alloy. Square and circle symbols are sine and cosine amplitude, respectively. (b) Phase of magnetization precession (φ) as a function of x extracted from (a).

on the simple dynamical model of magnetization ($\mathbf{m}$) and the induced OAM ($\delta\mathbf{L}$). Although *ab initio* theory of the inverse Faraday effect has been reported [29], the theory was calculated in a few compounds and derived to calculate OAM parallel to light propagation as well as magnetization direction for ferromagnets, which is different from the current experimental configuration. Therefore, we develop the model that allows us to consider precession of $\delta\mathbf{L}$ around magnetization considering $\delta\mathbf{L}$ generation owing to absorption of angular momentum where the framework of OAM generation was discussed in [37]. The torque equation for $\delta\mathbf{L}$ was derived from the Heisenberg equation of motion (see Sec. I-A in Supplemental Material [47]) in addition to OAM generation term and relaxation term as

$$\frac{\mathrm{d}\delta\mathbf{L}}{\mathrm{d}t} = \mathbf{Q}_\mathrm{L} - \xi'\delta\mathbf{L}\times\mathbf{m} - \frac{\delta\mathbf{L}}{\tau}, \tag{3}$$

where $\mathbf{Q}_\mathrm{L}$ is the generation rate of the electronic OAM and its sign depends on the photon helicity [Eq. (1)]. Note that the form of $\mathbf{Q}_\mathrm{L}$ in Eq. (3) is based on absorption effect, i.e., if there is no relaxation term OAM is preserved even after laser pulse passes away from the matter. As discussed in Fig. 1, we assume the relaxation time (τ) for the non-equilibrium OAM created and introduce SOC strength ξ' as the frequency dimension for the coupling between magnetization $\mathbf{m}$ and $\delta\mathbf{L}$. The timescale of dynamics induced by SOC and the relaxation process are shorter than pulse duration, thus we consider quasistationary state during the pulse duration. The steady state condition $\mathrm{d}(\delta\mathbf{L})/\mathrm{d}t = 0$ leads to a following equation:

$$\delta\mathbf{L} = \frac{\tau}{(\xi'\tau)^2+1}\mathbf{Q}_\mathrm{L} - \frac{\xi'\tau^2}{(\xi'\tau)^2+1}\mathbf{Q}_\mathrm{L}\times\mathbf{m} + \frac{(\xi'\tau)^2\tau}{(\xi'\tau)^2+1}(\mathbf{Q}_\mathrm{L}\cdot\mathbf{m})\mathbf{m}. \tag{4}$$

The first term represents the quasistatic electronic OAM whose direction is parallel to the light propagation direction and the second term arises from the rotation of OAM around $\mathbf{m}$ due to SOC between OAM and magnetization. The low-frequency dynamics of magnetization in ferromagnetic metals can be expressed using the Landau-Lifshitz equation with torque $\mathbf{T}$ as follows:

$$\frac{\mathrm{d}\mathbf{m}}{\mathrm{d}t} = -\gamma\mu_0\mathbf{m}\times\mathbf{H}_\mathrm{eff} + \mathbf{T}, \tag{5}$$

where, γ, μ_0, and $\mathbf{H}_\mathrm{eff}$ are the gyromagnetic ratio, vacuum permeability, and effective magnetic field, respectively. Here, we assume the torque is due to the SOC $\mathbf{T} = (\gamma\xi'/\mu_\mathrm{at})\mathbf{m}\times\delta\mathbf{L}$ (see Sec. I-A in [47]), where μ_at is the atomic magnetic moment. Then, we derived the following dynamical equation:

$$\frac{\mathrm{d}\mathbf{m}}{\mathrm{d}t} = -\gamma\mu_0\mathbf{m}\times\mathbf{H}_\mathrm{eff} + \frac{\gamma}{\mu_\mathrm{at}}\frac{\xi'\tau}{(\xi'\tau)^2+1}\mathbf{m}\times\mathbf{Q}_\mathrm{L} - \frac{\gamma}{\mu_\mathrm{at}}\frac{(\xi'\tau)^2}{(\xi'\tau)^2+1}\mathbf{m}\times(\mathbf{Q}_\mathrm{L}\times\mathbf{m}). \tag{6}$$

The second and third terms are the field and damping-like torques, respectively, and both are governed by the timescale of ξ' and τ, as discussed in Fig. 1. Here, laser was irradiated from the film normal; thus, $\mathbf{Q}_\mathrm{L} = -Q_\mathrm{L}\mathbf{z}$. Then, the field and damping-like torques were along the y and z directions. The z component magnetization precession amplitudes can be derived by impulsive response due to the torque $\mathbf{T}$ as [27]

$$\delta m_\mathrm{z,sin} = \frac{\gamma}{\mu_\mathrm{at}}\frac{\xi'\tau}{(\xi'\tau)^2+1}\beta Q_\mathrm{L}\Delta t, \tag{7}$$

$$\delta m_\mathrm{z,cos} = \frac{\gamma}{\mu_\mathrm{at}}\frac{(\xi'\tau)^2}{(\xi'\tau)^2+1}Q_\mathrm{L}\Delta t, \tag{8}$$

where Δt is the laser pulse duration. Here, we use $\mathbf{H}_\mathrm{eff} = H\mathbf{x} - M_\mathrm{eff}(\mathbf{m}\cdot\mathbf{z})\mathbf{z}$ with an external magnetic field (H) and effective demagnetizing field (M_eff). The factor $\beta = \sqrt{H/(H+M_\mathrm{eff})}$ is related to the elliptical shape of magnetization precession due to the demagnetizing field in the thin film.

The experimental and theoretical amplitudes are compared in Fig. 4(a). In this figure, we plot the normalized values of experimentally obtained magnetization precession amplitudes ($\mu_\mathrm{at}\delta m_\mathrm{z,sin}/\beta$ and $\mu_\mathrm{at}\delta m_\mathrm{z,cos}$) as functions of $\xi'\tau$. Here, we evaluated ξ' for Co-Pt alloy with different compositions (x) using the values of ξ' interpolation of the SOC strength energy for Co and Pt (Co: 0.085 eV, Pt: 0.72 eV) [59] with the well-known scaling rule $\sim Z_\mathrm{avg}^2$ [60],

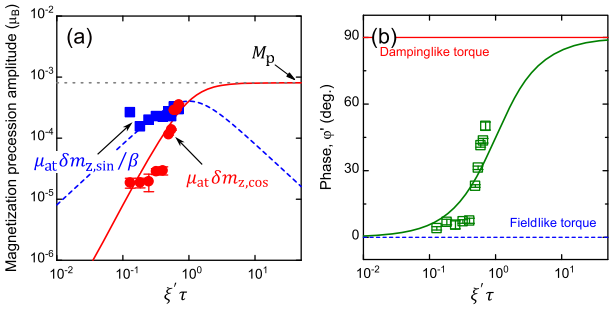

FIG. 4. (a) Magnetization precession amplitude ($\mu_\mathrm{at}\delta m_\mathrm{z,sin}/\beta$ and $\mu_\mathrm{at}\delta m_\mathrm{z,cos}$) and (b) phase [$\varphi'_\mathrm{exp} = \tan^{-1}(\beta\delta m_\mathrm{z,cos}/\delta m_\mathrm{z,sin})$] plotted as a function of $\xi'\tau$ in the model of photon-helicity–induced OAM transfer torque. Broken and solid curve in (a) are results calculated based on $M_\mathrm{p}\xi'\tau/[1+(\xi'\tau)^2]$ and $M_\mathrm{p}(\xi'\tau)^2/[1+(\xi'\tau)^2]$, respectively, where M_p corresponds to the orbital magnetization generated by light. Solid curve in (b) is the result calculated based on $\varphi'_\mathrm{the} = \tan^{-1}(\xi'\tau)$. Here, ξ scales with Z_ave^2 and orbital relaxation time τ of 1 fs.

where Z_{avg} is the average atomic number of Co-Pt alloy. We also set approximately used fixed value of $\tau \sim 1$ fs, which approximates photo-excited electron relaxation time, i.e., $\tau \sim 1$ fs for Co [61] (see Sec. IV in Supplemental Material for more detailed discussion for ξ' and τ for the alloys [47]). The theoretical curves in Eqs. (7) and (8) are shown with the broken and solid curves, respectively, in Fig. 4(a) under the assumption of a fixed value of $M_p = \gamma Q_L \Delta t \sim 0.8 \times 10^{-3}$ [μ_B]. The theoretical magnetization precession phase is given by the ratio between the field and damping-like torques in Eq. (6),

$$\varphi'_{the} = \tan^{-1}(\xi'\tau). \tag{9}$$

Figure 4(b) shows the theoretical and experimental phases of magnetization precession as a function of $\xi'\tau$. Here, experimental phase is corrected by the factor β, i.e., $\varphi'_{exp} = \tan^{-1}(\beta\delta m_{z,cos}/\delta m_{z,sin})$ from Eqs. (7) and (8) to compare with the theoretical phase φ'_{the} for the torques [Eq. (9)] In those figures, the experimental data for the amplitude and phase are in good agreement with those obtained from the theoretical model with the same footing.

The pertinent physics discussed thus far for helicity-induced magnetization dynamics is worth noting. As mentioned in the introduction, the inverse Faraday effect is traditionally considered to effectively generate magnetic fields in both magnetic metals and dielectrics owing to the magneto-optical coupling [10]. Thermodynamic considerations indicate that the effective magnetic field generated by the magneto-optical coupling is proportional to the Faraday or Kerr effect, which is characterized by magneto-optic constant Q. However, our sample showed a reduction of the Kerr effect with an increase in the Pt concentration, contrary to the significant increase in helicity-induced torque with increasing Pt concentration(see Secs. II-A and V-A in Supplemental Material [47]). Thus, significant increase of both field and damping-like torques with Pt concentration cannot be explained by the inverse Faraday effect due to magneto-optical coupling. On the other hand, recent microscopic theories facilitated further understanding of the nature of field and damping-like torques in metals via SAM directed to $\delta\mathbf{S}$ and $\delta\mathbf{S} \times \mathbf{m}$, respectively, where $\delta\mathbf{S}$ is SAM induced by the circularly polarized light [33]. The theoretical computations predicted that field-like torque was significantly enhanced in ferromagnetic metals with large SOC such as FePt, with the damping-like torque being much smaller than the field-like torque. Concerning the SAM generation, the emergence of the damping-like torque with increasing Pt concentration is difficult to be interpreted as the SAM generation in ferromagnets, i.e., $\mathbf{M}_p \sim \delta\mathbf{S}$ in Eq. (1), similar to that observed in GaMnAs [62]. When $\delta\mathbf{S}$ is generated by circularly polarized light irradiation, the timescale is characterized by the exchange coupling (J_{ex}) of the induced $\delta\mathbf{S}$ and $\mathbf{m}$, and relaxation time of the induced spin (τ_S). Hence, we can expect $\varphi \sim \tan^{-1}(J_{ex}\tau_S/\hbar)$, similar to Eq. (9). It is difficult to consider that the phase increases with increasing Pt concentration (x) in Co-Pt alloys because Pt addition would deteriorate ferromagnetism, that is, reduction of J_{ex}. Also, Pt addition reduces τ_S due to its strong SOC according to the Elliot-Yafet mechanism [63]. Similarly, the damping-like torque has been discussed in terms of the SAM induced in the heavy metals in ferromagnet and heavy-metal bilayers; however, the physics behind this torque is related to the spin-transfer torque owing to the SAM flow in the bilayer [25]. Moreover, ultrafast damping-like torque was observed in antiferromagnet [16]. This was caused by the exchange enhancement of the Gilbert damping torque, which may be a unique feature in some antiferromagnets and not the case in ferromagnets studied here (see Sec. V-B in Supplemental Material [47] for detailed discussion). Thus, we ruled out the physical mechanisms of the damping-like torque proposed to date.

Our Letter indicates that the OAM induced by light plays a much more important role than the SAM induced by the light. We try to quantify generation of OAM and orbital magnetization owing to light absorption in metals [37]. The calculation of $\mathbf{M}_p$ generated due to conservation of angular momentum leads to a value $\sim 10^{-2}$ [μ_B] one order of magnitude larger than that used to explain the experimental result $\sim 10^{-3}$ [μ_B] [Fig. 4(a) and see Sec. VI in Supplemental Material [47] for detailed calculation]. This fact indicates that some part of the induced OAM contributes to the magnetization torque. It is likely that the torque may dominantly be caused by the induced OAM with d-electron character since magnetization is mostly composed of the d electron. On the other hand, conservation law accounts induced OAM for sp electrons as well as that for the d electron, which might be a source of the difference between experiment and calculation based on the conservation law. Thus, for a more quantitative discussion, we need the quantum theory of the angular momentum dynamics and torque induced by light, taking account of realistic band structure beyond the naive phenomenological model discussed here, which is out of scope of the Letter and will be a subject for future works.

In summary, we investigated helicity-dependent laser-induced magnetization precession in $Co_{1-x}Pt_x$ alloys. We demonstrated that the magnitude and the phase of the magnetization precession induced by the circularly polarized laser pulse systematically increase with the Pt concentrations in the $Co_{1-x}Pt_x$ alloy film. Those evolutions are attributed to two different types of induced torques: field and damping-like torques. The experimental data are well-described by a simple model that considers the electronic OAM generated by light and its coupling with magnetization via SOC. This Letter deepens the understanding of the physics relevant to the interaction with photon helicity and matter. Furthermore, this Letter opens alternative route for manipulating magnetization in magnetic substances.

Acknowledgments—This work was supported by Grants-in-Aid for Scientific Research (No. 21H04648 and No. 21H05000), Grant-in-Aid for Challenging Research (No. 24K21234), Grant-in-Aid for Transformative Research Areas (No. 24H02235), JST PRESTO (No. JPMJPR22B2), X-NICS of MEXT (No. JPJ011438), CSIS cooperative research project in Tohoku University, the Asahi Glass Foundation, the Murata Science Foundation, Advanced Technology Institute Research Grants, FRIS Creative Interdisciplinary Collaboration Program in Tohoku University. This work was also supported by the ANR-20-CE09-0013 UFO, by "Lorraine Université d'Excellence" reference ANR-15-IDEX-04-LUE, and by the French National Research Agency through the France 2030 government grants PEPR Electronic EMCOM (ANR-22-PEEL-0009). S. I. thanks to TI-FRIS fellowship at Tohoku University. K. N. and K. I. thank to GP-Spin at Tohoku University. S. M. thanks to CSRN of CSIS at Tohoku University. The authors thank Gyung-Min Choi for valuable discussion.

[1] K. Y. Bliokh, F. J. Rodríguez-Fortuño, F. Nori, and A. V. Zayats, Spin-orbit interactions of light, Nat. Photonics **9**, 796 (2015).

[2] K. Y. Bliokh and F. Nori, Transverse and longitudinal angular momenta of light, Phys. Rep. **592**, 1 (2015).

[3] T. Omatsu, K. Chujo, K. Miyamoto, M. Okida, K. Nakamura, N. Aoki, and R. Morita, Metal microneedle fabrication using twisted light with spin, Opt. Express **18**, 17967 (2010).

[4] K. Toyoda, K. Miyamoto, N. Aoki, R. Morita, and T. Omatsu, Using optical vortex to control the chirality of twisted metal nanostructures, Nano Lett. **12**, 3645 (2012).

[5] A. E. Willner, K. Pang, H. Song, K. Zou, and H. Zhou, Orbital angular momentum of light for communications, Appl. Phys. Rev. **8**, 041312 (2021).

[6] Z. Ji, W. Liu, S. Krylyuk, X. Fan, Z. Zhang, A. Pan, L. Feng, A. Davydov, and R. Agarwal, Photocurrent detection of the orbital angular momentum of light, Science **368**, 763 (2020).

[7] J. Ishihara, T. Mori, T. Suzuki, S. Sato, K. Morita, M. Kohda, Y. Ohno, and K. Miyajima, Imprinting spatial helicity structure of vector vortex beam on spin texture in semiconductors, Phys. Rev. Lett. **130**, 126701 (2023).

[8] J. P. van der Ziel, P. S. Pershan, and L. D. Malmstrom, Optically-induced magnetization resulting from the inverse Faraday effect, Phys. Rev. Lett. **15**, 190 (1965).

[9] P. S. Pershan, J. P. van der Ziel, and L. D. Malmstrom, Theoretical discussion of the inverse Faraday effect, Raman scattering, and related phenomena, Phys. Rev. **143**, 574 (1966).

[10] A. Kirilyuk, A. V. Kimel, and T. Rasing, Ultrafast optical manipulation of magnetic order, Rev. Mod. Phys. **82**, 2731 (2010).

[11] A. V. Kimel, A. Kirilyuk, P. A. Usachev, R. V. Pisarev, A. M. Balbashov, and T. Rasing, Ultrafast non-thermal control of magnetization by instantaneous photomagnetic pulses, Nature (London) **435**, 655 (2005).

[12] T. Satoh, S. J. Cho, R. Iida, T. Shimura, K. Kuroda, H. Ueda, Y. Ueda, B. A. Ivanov, F. Nori, and M. Fiebig, Spin oscillations in antiferromagnetic NiO triggered by circularly polarized light, Phys. Rev. Lett. **105**, 077402 (2010).

[13] T. Satoh, Y. Terui, R. Moriya, B. A. Ivanov, K. Ando, E. Saitoh, T. Shimura, and K. Kuroda, Directional control of spin-wave emission by spatially shaped light, Nat. Photonics **6**, 662 (2012).

[14] G. M. Choi, A. Schleife, and D. G. Cahill, Optical-helicity-driven magnetization dynamics in metallic ferromagnets, Nat. Commun. **8**, 15085 (2017).

[15] I. V. Savochkin, M. Jäckl, V. I. Belotelov, I. A. Akimov, M. A. Kozhaev, D. A. Sylgacheva, A. I. Chernov, A. N. Shaposhnikov, A. R. Prokopov, V. N. Berzhansky, D. R. Yakovlev, A. K. Zvezdin, and M. Bayer, Generation of spin waves by a train of fs-laser pulses: A novel approach for tuning magnon wavelength, Sci. Rep. **7**, 5668 (2017).

[16] C. Tzschaschel, T. Satoh, and M. Fiebig, Efficient spin excitation via ultrafast damping-like torques in antiferromagnets, Nat. Commun. **11**, 6142 (2020).

[17] C. H. Lambert, S. Mangin, B. S. S. Varaprasad, Y. K. Takahashi, M. Hehn, M. Cinchetti, G. Malinowski, K. Hono, Y. Fainman, M. Aeschlimann, and E. E. Fullerton, All-optical control of ferromagnetic thin films and nanostructures, Science **345**, 1337 (2014).

[18] M. S. El Hadri, P. Pirro, C.-H. Lambert, S. Petit-Watelot, Y. Quessab, M. Hehn, F. Montaigne, G. Malinowski, and S. Mangin, Two types of all-optical magnetization switching mechanisms using femtosecond laser pulses, Phys. Rev. B **94**, 064412 (2016).

[19] R. Medapalli, D. Afanasiev, D. K. Kim, Y. Quessab, S. Manna, S. A. Montoya, A. Kirilyuk, T. Rasing, A. V. Kimel, and E. E. Fullerton, Multiscale dynamics of helicity-dependent all-optical magnetization reversal in ferromagnetic Co/Pt multilayers, Phys. Rev. B **96**, 224421 (2017).

[20] Y. K. Takahashi, R. Medapalli, S. Kasai, J. Wang, K. Ishioka, S. H. Wee, O. Hellwig, K. Hono, and E. E. Fullerton, Accumulative magnetic switching of ultrahigh-density recording media by circularly polarized light, Phys. Rev. Appl. **6**, 054004 (2016).

[21] R. John, M. Berritta, D. Hinzke, C. Müller, T. Santos, H. Ulrichs, P. Nieves, J. Walowski, R. Mondal, O. Chubykalo-Fesenko, J. McCord, P. M. Oppeneer, U. Nowak, and M. Münzenberg, Magnetisation switching of FePt nanoparticle recording medium by femtosecond laser pulses, Sci. Rep. **7**, 4114 (2017).

[22] G. Kichin, M. Hehn, J. Gorchon, G. Malinowski, J. Hohlfeld, and S. Mangin, From multiple- to single-pulse all-optical helicity-dependent switching in ferromagnetic Co/Pt multilayers, Phys. Rev. Appl. **12**, 024019 (2019).

[23] F. Cheng, Z. Du, X. Wang, Z. Cai, L. Li, C. Wang, A. Benabbas, P. Champion, N. Sun, L. Pan, and Y. Liu, All-optical helicity-dependent switching in hybrid metal–ferromagnet thin films, Adv. Opt. Mater. **8**, 2000379 (2020).

[24] G. M. Choi, H. G. Park, and B. C. Min, The orbital moment and field-like torque driven by the inverse Faraday effect in metallic ferromagnets, J. Magn. Magn. Mater. **474**, 132 (2019).

[25] G. M. Choi, J. H. Oh, D. K. Lee, S. W. Lee, K. W. Kim, M. Lim, B. C. Min, K. J. Lee, and H. W. Lee, Optical spin-orbit torque in heavy metal-ferromagnet heterostructures, Nat. Commun. **11**, 1482 (2020).
[26] S. Iihama, K. Ishibashi, and S. Mizukami, Interface-induced field-like optical spin torque in a ferromagnet/heavy metal heterostructure, Nanophotonics **10**, 1169 (2021).
[27] S. Iihama, K. Ishibashi, and S. Mizukami, Photon spin angular momentum driven magnetization dynamics in ferromagnet/heavy metal bilayers, J. Appl. Phys. **131**, 023901 (2022).
[28] C. Wang, Y. Xu, and Y. Liu, Photon energy-dependent optical spin-orbit torque in heavy metal–ferromagnet bilayers, Adv. Funct. Mater. **34**, 2307753 (2023).
[29] M. Berritta, R. Mondal, K. Carva, and P. M. Oppeneer, *Ab initio* theory of coherent laser-induced magnetization in metals, Phys. Rev. Lett. **117**, 137203 (2016).
[30] R. Hertel, Theory of the inverse Faraday effect in metals, J. Magn. Magn. Mater. **303**, L1 (2006).
[31] D. Popova, A. Bringer, and S. Blügel, Theoretical investigation of the inverse Faraday effect via a stimulated Raman scattering process, Phys. Rev. B **85**, 094419 (2012).
[32] R. Mondal, M. Berritta, C. Paillard, S. Singh, B. Dkhil, P. M. Oppeneer, and L. Bellaiche, Relativistic interaction Hamiltonian coupling the angular momentum of light and the electron spin, Phys. Rev. B **92**, 100402(R) (2015).
[33] F. Freimuth, S. Blügel, and Y. Mokrousov, Laser-induced torques in metallic ferromagnets, Phys. Rev. B **94**, 144432 (2016).
[34] J. Li and P. M. Haney, Optical spin transfer and spin-orbit torques in thin-film ferromagnets, Phys. Rev. B **96**, 054447 (2017).
[35] P. Scheid, G. Malinowski, S. Mangin, and S. Lebègue, *Ab initio* theory of magnetization induced by light absorption in ferromagnets, Phys. Rev. B **100**, 214402 (2019).
[36] S. B. Mishra and S. Coh, Spin contribution to the inverse Faraday effect of nonmagnetic metals, Phys. Rev. B **107**, 214432 (2023).
[37] P. Scheid, S. Mangin, and S. Lebègue, Light-absorbed orbital angular momentum in the linear response regime, arXiv:2311.1477.
[38] P. Scheid, S. Sharma, G. Malinowski, S. Mangin, and S. Lebègue, *Ab initio* study of helicity-dependent light-induced demagnetization: From the optical regime to the extreme ultraviolet regime, Nano Lett. **21**, 1943 (2021).
[39] P. Scheid, Q. Remy, S. Lebègue, G. Malinowski, and S. Mangin, Light induced ultrafast magnetization dynamics in metallic compounds, J. Magn. Magn. Mater. **560**, 169596 (2022).
[40] D. Go and H. W. Lee, Orbital torque: Torque generation by orbital current injection, Phys. Rev. Res. **2**, 013177 (2020).
[41] D. Go, F. Freimuth, J.-P. Hanke, F. Xue, O. Gomonay, K.-J. Lee, S. Blügel, P. M. Haney, H.-W. Lee, and Y. Mokrousov, Theory of current-induced angular momentum transfer dynamics in spin-orbit coupled systems, Phys. Rev. Res. **2**, 033401 (2020).
[42] S. Ding, A. Ross, D. Go, L. Baldrati, Z. Ren, F. Freimuth, S. Becker, F. Kammerbauer, J. Yang, G. Jakob, Y. Mokrousov, and M. Kläui, Harnessing orbital-to-spin conversion of interfacial orbital currents for efficient spin-orbit torques, Phys. Rev. Lett. **125**, 177201 (2020).
[43] S. Lee, M. G. Kang, D. Go, D. Kim, J. H. Kang, T. Lee, G. H. Lee, J. Kang, N. J. Lee, Y. Mokrousov, S. Kim, K. J. Kim, K. J. Lee, and B. G. Park, Efficient conversion of orbital Hall current to spin current for spin-orbit torque switching, Commun. Phys. **4**, 234 (2021).
[44] D. Lee, D. Go, H. J. Park, W. Jeong, H. W. Ko, D. Yun, D. Jo, S. Lee, G. Go, J. H. Oh, K. J. Kim, B. G. Park, B. C. Min, H. C. Koo, H. W. Lee, O. J. Lee, and K. J. Lee, Orbital torque in magnetic bilayers, Nat. Commun. **12**, 6710 (2021).
[45] Y. G. Choi, D. Jo, K. H. Ko, D. Go, K. H. Kim, H. G. Park, C. Kim, B. C. Min, G. M. Choi, and H. W. Lee, Observation of the orbital Hall effect in a light metal Ti, Nature (London) **619**, 52 (2023).
[46] H. Hayashi, D. Jo, D. Go, T. Gao, S. Haku, Y. Mokrousov, H. W. Lee, and K. Ando, Observation of long-range orbital transport and giant orbital torque, Commun. Phys. **6**, 32 (2023).
[47] See Supplemental Material at http://link.aps.org/supplemental/10.1103/PhysRevLett.134.016701 for derivation of equations, materials properties of Co-Pt alloy, all data of photon-helicity–induced magnetization dynamics, parameters used in the model calculation, model calculations with other possible scenario, and calculation of orbital angular momentum generation, which includes Refs. [48–58].
[48] I. H. Malitson, Interspecimen comparison of the refractive index of fused silica, J. Opt. Soc. Am. **55**, 1205 (1965).
[49] M. A. Green, Self-consistent optical parameters of intrinsic silicon at 300 K including temperature coefficients, Sol. Energy Mater. Sol. Cells **92**, 1305 (2008).
[50] I. H. Malitson, Refraction and dispersion of synthetic sapphire, J. Opt. Soc. Am. **52**, 1377 (1962).
[51] P. B. Johnson and R. W. Christy, Optical constants of transition metals: Ti, V, Cr, Mn, Fe, Co, Ni, and Pd, Phys. Rev. B **9**, 5056 (1974).
[52] Optical data from Sopra SA, https://www.sspectra.com/sopra.html.
[53] B. Heinrich, J. F. Cochran, M. Kowalewski, J. Kirschner, Z. Celinski, A. S. Arrott, and K. Myrtle, Magnetic anisotropies and exchange coupling in ultrathin fcc Co(001) structures, Phys. Rev. B **44**, 9348 (1991).
[54] F. D. Longa, J. T. Kohlhepp, W. J. M. de Jonge, and B. Koopmans, Influence of photon angular momentum on ultrafast demagnetization in nickel, Phys. Rev. B **75**, 224431 (2007).
[55] S. Iihama, Y. Sasaki, H. Naganuma, M. Oogane, S. Mizukami, and Y. Ando, Ultrafast demagnetization of $L1_0$ FePt and FePd ordered alloys, J. Phys. D **49**, 035002 (2015).
[56] E. Zarate, P. Apell, and P. M. Echenique, Calculation of low-energy-electron lifetimes, Phys. Rev. B **60**, 2326 (1999).
[57] J. J. Krebs, G. A. Prinz, D. W. Forester, and W. G. Maisch, Magneto-optical characterization of thin films of $Fe_{1-x}B_x$, $Fe_{1-x}Si_x$ and Fe-overcoated permalloy, J. Appl. Phys. **50**, 2449 (1979).

[58] J. Zak, E. R. Moog, C. Liu, and S. D. Bader, Universal approach to magneto-optics, J. Magn. Magn. Mater. **89**, 107 (1990).

[59] O. Šipr, J. Minár, S. Mankovsky, and H. Ebert, Influence of composition, many-body effects, spin-orbit coupling, and disorder on magnetism of Co-Pt solid-state systems, Phys. Rev. B **78**, 144403 (2008).

[60] K. V. Shanavas, Z. S. Popović, and S. Satpathy, Theoretical model for Rashba spin-orbit interaction in d electrons, Phys. Rev. B **90**, 165108 (2014).

[61] M. Bauer, A. Marienfeld, and M. Aeschlimann, Hot electron lifetimes in metals probed by time-resolved two-photon photoemission, Prog. Surf. Sci. **90**, 319 (2015).

[62] P. Němec, E. Rozkotová, N. Tesařová, F. Trojánek, E. D. Ranieri, K. Olejník, J. Zemen, V. Novák, M. Cukr, P. Malý, and T. Jungwirth, Experimental observation of the optical spin transfer torque, Nat. Phys. **8**, 411 (2012).

[63] I. Žutić, J. Fabian, and S. D. Sarma, Spintronics: Fundamentals and applications, Rev. Mod. Phys. **76**, 323 (2004).